Fabrication Of Photovoltaic Thread Using N-Type Tungsten Oxide

By

Audriy Jebet

Submitted In Partial Fulfilment Of The Requirements

for the Degree of

Master of Science

in the

Chemistry

Program

YOUNGSTOWN STATE UNIVERSITY

May, 2020

Fabrication Of Photovoltaic Thread Using N-Type Tungsten Oxide		
Audriy Jebet		
I hereby release this thesis to the public. I understand that this thesis will be made available from the OhioLINK ETD Center and the Maag Library Circulation Desk for public access. I also authorize the University or other individuals to make copies of this thesis as needed for scholarly research.		
Signature :		
	_____ *Audriy Jebet, Student*	_____ Date
Approvals:		
	_____ *Dr. Clovis A. Linkous*, Thesis Advisor	_____ Date
	_____ *Dr. Sherri Lovelace - Cameron*, Committee Member	_____ Date
	_____ *Dr. Christopher Arntsen*, Committee Member	_____ Date
	_____ Dr. Salvatore A. Sanders, Dean of Graduate of Studies	_____ Date

Acknowledgements

.

First, I would like to thank my advisor Dr. Linkous for giving me the opportunity to undertake this project and his unconditional trust upon me. Thank you, Dr. Sherri Lovelace – Cameron and Dr. Christopher Arntsen, for being on my thesis committee.

Special thanks to my research group members: Milica, Omweri, Kim and Malika, it's been a pleasure working with you all. I would like to thank Ray Hoff for SEM and XRD training.

I would like to thank my family for the emotion support during this entire period.

Finally, I wish to dedicate this thesis to Kevin Rono for his collaborative inputs.

Abstract

The concept of photovoltaic clothing is currently not popular because of challenges like cost, reliability and the availability of flexible photovoltaic devices that could be integrated into fabrics. Tungsten oxide is a wide band gap (2.6 eV) n-type semiconductor, which has a wide range of pH stability and also a high melting point. The current study presents the cathodic electrodeposition of WO_3 in a variety of conditions on three types of substrates: Fluorine tin oxide (FTO), stainless steel-304 and tungsten foil. The surface morphology of the elctrodeposited WO_3 was investigated using SEM. XRD was used to explore the crystallinity of the solid material and the photoactivity was tested using a xenon lamp solar simulator and a potentiostat. A profilometer was used to measure the thickness of the films. The samples were annealed in air at 450 ˚C for 2 h. The monoclinic phase of WO_3 was synthesized and the thickness of the film ranged between 400-518 nm. WO_3 on FTO substrate produced a photocurrent of 14.4 μA /cm^2 and photovoltage of 658 mV using the oxygen evolution method. WO_3 on W foil substrate was able to registered a photocurrent of 39.3 μA /cm^2 and a voltage of 971 mV photoactivity. It was evident from the results that the stability of the substrate under different pH conditions plays a great role in enabling photoactivity.

Table of Content

List of Figures

CHAPTER ONE

Introduction

Global climate change and depletion of oil has led to advances in research in the generation of electricity using renewable sources [1]. The energy sector has focused on curbing these shortcomings by turning to solar cells [1-2]. Renewable energy sources are sources which can be regenerated, hence do not undergo depletion. They include: wind, water, geothermal and solar energy [2]. In 2018, about 17% of electricity generation in the USA came from renewable energy sources, in which 1.5% came from solar cells [3]. In a year, the sun produces about 1.38×10^6 exajoules of energy, which is 2500 times more than what is consumed by human activity on earth [4]. This energy can be converted into accessible forms like electricity, thermal energy, biofuels and fuels like hydrogen via water-splitting processes [4].

Photovoltaic cells

The energy from the sun can be converted directly into electricity through a phenomenon known as the photovoltaic effect [5]. The photovoltaic effect occurs when sunlight irradiates the material used in a photovoltaic cell, causing a photo-potential [5]. It was first discovered by Becquerel while experimenting with a solid electrode in an electrolyte solution [5-6]. He placed two platinuim electrodes in an electrolyte containing a metal halide salt, and upon illumination he produced a current [6].

Currently there are various semiconductors that exhibit photoconductive properties. They include group II-VI and group III-V elements [5-6]. Photovoltaic cells are becoming more popular because they now have a long life span of about 20-30 years and produce a clean form of energy [7].

It is estimated that by 2030, one terawatt of energy could be from photovoltaic cells worldwide [1]. Most development of photovoltaic cells is focused on striking a balance between the cost of production of the cell and efficency. Also the flexibility of the material is taken into account [8]. The traditional wafer-based silicon cells are known to have good efficiency of 15-18%; however, they are very expensive and rigid [1]. This has led to development of thin film solar cells with moderate efficiency; however they suffer from various shortcomings. For instance, cadmium telluride, which has efficieny of 6-9%, is very poisonous [8]. Copper indium diselenide (CIS) has a greater efficiency of 7.5-9.5%, but indium is very rare [8].

There has been a lot of progress in photovoltaic technology, leading to the development of other cells that are easy to fabricate. They include copper zinc tin sulfide (CZTS), dye-sensitized solar cells (DSSC), perovskites, organic and quantum dot solar cells [3,8]. These cells have high efficiencies; for instance, an efficiency of 12.8% have been achieved with CZTS [9]. Perovskite cells on the other hand have risen from 3.8% in 2009 to 24.2% in 2019 [3]. Despite having high efficiencies, these cells are yet to be commercialized because they suffer from low open circuit voltage [3].

The Schockley-Queisser limit

The Schockley-Queisser limit is the maximum theoretical efficiency of a solar cell made from a single p-n junction as a function of band gap energy. It is obtained by determining the amount of electrical energy that a single photon produces[10].

For a single -junction semiconductor, with a band gap energy of 1.34 eV, the energy conversion efficiency is 33.7 % using the AM 1.5 solar spectrum. It is the standard to which efficiencies of emerging solar cells are compared[10].

The Shockley -Queisser limit is based on the following conditions:

i. Each incoming photon excites only one electron-hole pair

ii. The solar cell material consists of a single band gap energy

iii. Photons with energy lower than band gap energy are not absorbed while those with energy greater than band gap are absorbed. Any excess energy is transferred to the generated electron-hole pair and is lost through thermal relaxation.

iv. An infinite mobility of charge carriers.

v. Loss of electron-hole pairs is through radiative recombination only

vi. Illumination of the solar cell is by unconcentrated sunlight under standard test conditions (AM 1.5, 1000 W/m^2 and 300 K or 27 °C cell temperature)

vii. The sun is a black body at 6000 K, and the solar cell is a black body at 300 K

Tungsten oxide has a solar conversion efficiency which lies in the 5-10% range according to the Shockley-Queisser limit, as shown in Figure 1.

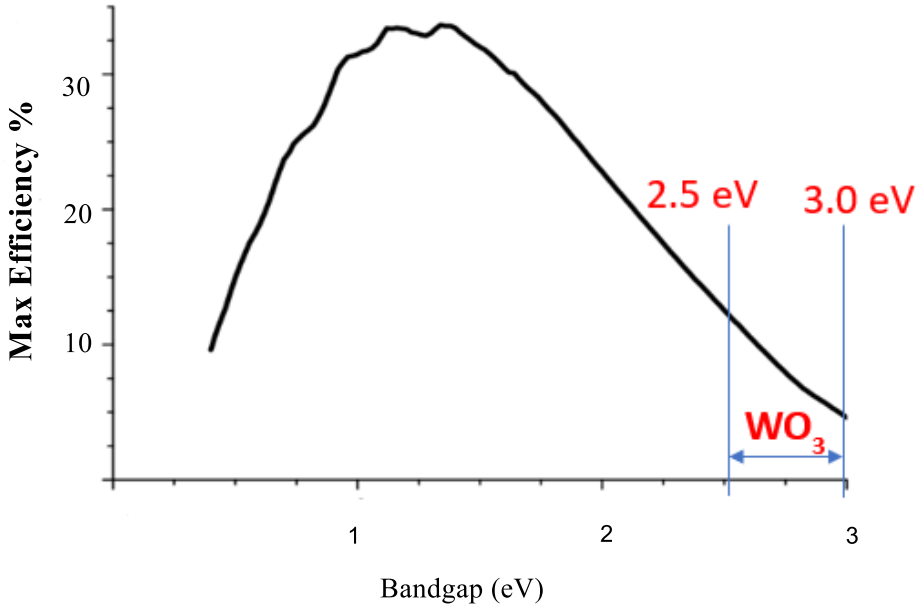

Figure 1: Schockely-Queissner plot of solar efficiency vs band gap energy [10]

Photovoltaic clothing

One of the ways to make a photovoltaic cloth in future will be attaching microscopic photovoltaic cells to woven fabric to produce energy. Textile fibers are 10-40 μm thick and are twisted together to form yarn, which is then woven to form a fabric [11].

The fabric is made electrically conductive by either intertwining conducting yarns into a fabric or depositing a thin conducting film on the fabric. Ink-jet printing is the commonly used method: conductive ink is deposited on the fabric, and then compacted. Other methods include screen printing and metal coating techniques [11].

Photovoltaic clothing technology, which is still in the introductory stage, is becoming popular due to the possibility of incorporating flexibility into the clothing [12].

Tungsten oxide

Tungsten oxides (WO_X) were first synthesized in the 17^{th} century from $LiWO_3$ [13]. They are popular for their chromism, photocatalysis, and sensing applications. Recent research on tungsten oxide has focused on developing a photovoltaic cell using it as a semiconductor material [13]. ZnO and TiO_2 are common metal oxides that have been used in solar cells [13]. They have band gap energies of 3.37 and 3.2 eV, respectively, hence utilizing 5% of the solar energy, which represents the ultraviolet region [14]. Tungsten oxide is well known as an n-type semiconductor that has a band gap energy that ranges from 2.4 - 2.8 eV. It also has the advantage of being stable in different pH conditions and temperatures [15].

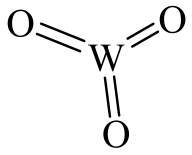

Figure 2: Tungsten oxide

Band gap Energy

The electronic band gap energy is the difference between the upper and lower energy levels of the valence and conduction bands [16]. A semiconductor in the ground state has electrons in the valence band, whereas the conduction band is empty [16]. During illumination, if the photon energy is greater than the band gap energy of the semiconductor, an electron in the valence band is excited to the conduction band; at the same time, a hole remains in the valence band [11,14].

In WO_3 the electronic bandgap (E_g) is characterized by the difference between the energy levels of the valence band, formed by filled O-2p orbitals, and the conduction band, formed by empty W-5d orbitals [13]. Thus, the distortion of WO_3 symmetry from the ideal cubic phase has an impact on the electronic band gap, since the occupied levels of the W 5d states are affected [17]. Studies show that amorphous tungsten trioxide possesses the largest band gap, while the monoclinic phase at room temperature has the lowest [17].

The ability of a material to absorb light in the visible region of the electromagnetic spectrum depends on its energy band gap [13].

Stoichiometric WO_3 is nearly transparent to visible light, thus possessing a slight yellow color. Non-stoichiometric WO_X exhibits light green color, due to the extra absorption peak tailing into the visible region from the infrared region, caused by transfer of an electron onto W^{6+} to make W^{5+} [13].

Doping

Doping involves the addition of a different element into the semiconductor so as to improve its properties [13], [16]. The electronic properties of tungsten oxide are altered when Li^+, H^+ or Na^+ is intercalated into it [13]. The s-orbital of Li and Na dopants is above the W 5d orbital of the WO_3 conduction band. This increases free electron density, which in turn induces metallic properties [13].

Studies shows that N-doping of tungsten oxide also reduces the band gap energy. Makorov et al [18] reported that the addition of Al_2O_3 to the tungsten oxide film enhances its electrical conductiviy. Other metal oxides that have been added to improve the conductivity include: TiO_2, Co_3O_4 and MnO_2 [13].

Tungsten oxide can be easily made into an n-type semiconductor, as oxygen lattice vacancies contain non-bonding electrons, which can be promoted to the conduction band and become the majority charge carrier [16]. Doping affects the distribution of electrons in WO_3, thus making its Fermi energy to be below the conduction band. In solid state materials, the Fermi level is the energy level at which the probability of finding an electron is 50% [16].

Annealing WO_3 at different temperatures results in the insertion of oxygen into its lattice, hence causing tilting and shifting distortions of W from the center of octahedra [11,15]. It has a great impact on the symmetry of the tungsten oxide. Depending on the magnitude of these distortions and temperatures, WO_3 undergoes different phase transitions[13]. Annealing of WO_3 film is vital for solar application. Photocurrent conversion effiency increases and the band gap energy is lowered when an annealed electrode is used for photoelectrochemical conversion. Studies have reported that an optimium photoactivity was achieved when a WO_3 film annealed at 450 ˚C was used [19].

Solid-liquid junctions interface

At the semiconductor and electrolyte interface, the redox potential of the solution and the Fermi energy level plays an important role. The Fermi level of n-type semiconductor is higher than the redox potential of the electrolyte [16]. The electrons, which are majority charge carriers, are transferred from the electrode into the solution.The positive charges in the space charge region causes the band edge to bend upward (figure 2) [16]. Band bending is a phenomena that occurs when an electric field is applied to a semiconductor [16]

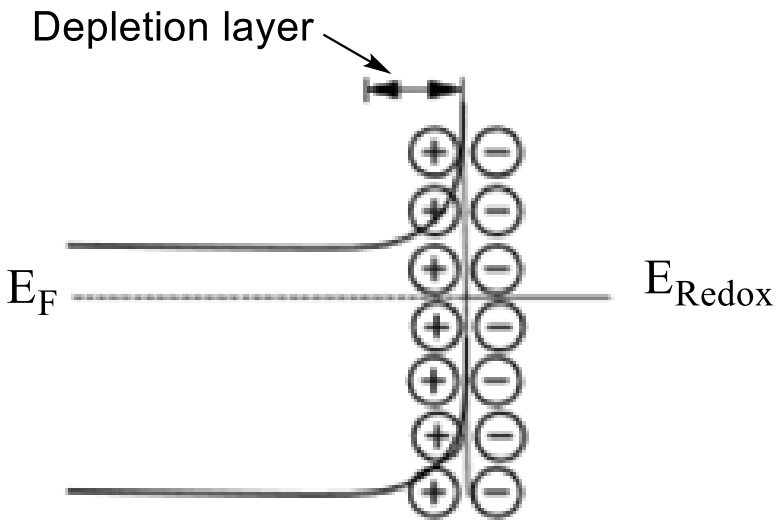

Figure 3: Band bending for an n-type semiconductor[16]

The applied potential on the electrolyte has an impact on the band edge of the the semiconductor. Varying the applied potential can result in three conditions:-Flat band potential, depletion region and accumulation region.

Flat band potential, Figure 4(a), occurs when the Fermi energy lies at the same energy as the solution redox potential, so there is no net transfer of charge. Depletion regions occur, as shown in Figure 4(b), when potential is positive with respect to the flat band potential. An accumulation region, Figure 4(c), occurs when the potential is negative with respect to the flat band [16].

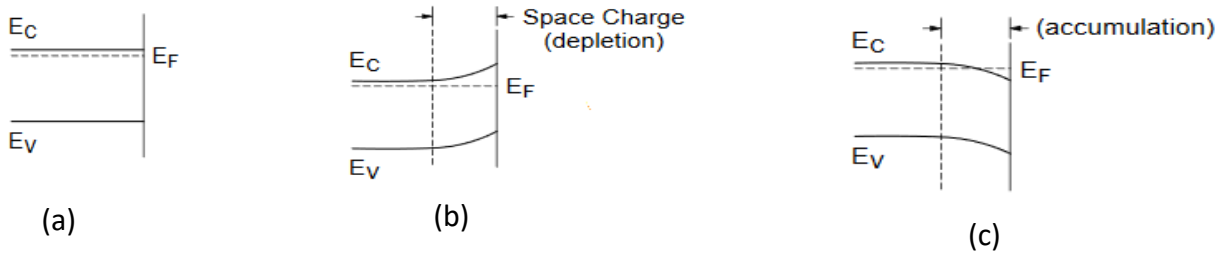

Figure 4: Effect of varying the applied potential (E) on the band edges of an n-type semiconductor. (a) $E=E_{fb,}$ (b) $E > E_{fb}$, (c) $E < E_{fb}$[16]

As shown in Figure 5, when the potential is swept negative with respect to the flat band potential, an accumulation region, region I, makes the semiconductor to show metallic characteristics, hence enabling charge tranfers both in the dark and in the light [16]. However, when it is swept positive, a depletion region, region III, occurs thus hindering the charge transfer and no voltage or current is exhibited in the dark. When illuminated, a photocurrent can be observed [16].

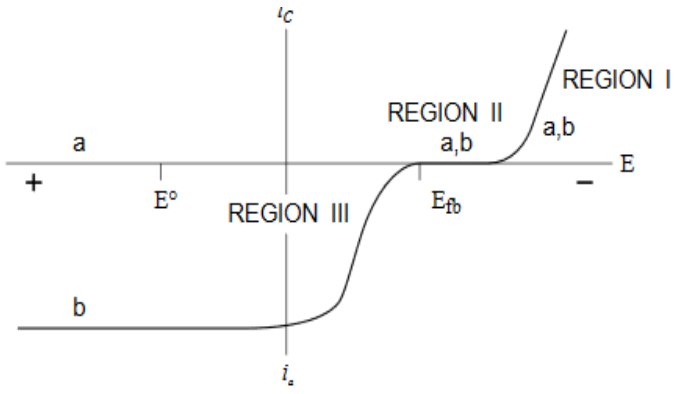

Figure 5: Ideal behavior for an n-type semiconductor (a) in the dark and (b) under irradiation [16]

Electrodeposition

There are several methods that have been used to synthesize thin films of tungsten oxides. They include: chemical vapor deposition, sputtering and screen printing [20]. However, they are costly and involve cumbersome processes in depositing onto a substrate. Electrodeposition is a simple and cheap method; it also enables the tailoring the film thickness by varying deposition conditions: time and voltage [19].

Cathodic electrodeposition of WO_3 works by increasing the pH near the surface of the electrode, which results in the decomposition of peroxotungstate ion, $W_2O_{11}^{2-}$, under reduction to form tungsten oxide [19].

General cathodic electrodeposition of WO_3 on a substrate can be described by the equation below:

$$W_2O_{11}^{2-} + 2(x+1)H^+ + 2xe^- \longrightarrow 2WO_3 + (x+1)H_2O + (4-x/2)O_2$$

Where: x = 1, 2, 3 or 4

Yamanaka and his group [21] were the first to synthesize tungsten oxide film through cathodic electrodeposition. They mixed colloidal tungstic acid with hydrogen peroxide. A platinum electrode was used to eliminate the excess hydrogen peroxide to form the peroxotungstate species. However, this method suffered from instability of the peroxo-compounds, which underwent decomposition after 3 - 4 hours. Shen *et al*[22] was able to improve the stability by adding alcohol to the precursor solution; The pH of the precursor solution has an impact on the morphology of the film formed. Studies have also revealed that mesoporous tungsten oxide films tend to have better photoactivity properties compared to their thin solid film counterparts [15].

Electrodeposition of tungsten oxide has been done on different substrates. Indium-doped tin oxide (ITO) and the fluorine-doped tin oxide (FTO) film on glass electrodes are the most popular. In their research Shen and Tseng [22] concluded that the WO_3 oxide film had the highest coverage on ITO film, gold foil and platinum foil respectively.

Baeck et al [23] were able to synthesis films with high current densities on titanium electrodes compared to the tungsten oxide electrode [23].

For this work, a quick and simple electrodeposition method established by Pauporte [24] was adopted, in which a Na_2WO_4 solution was mixed with 30% H_2O_2 and adjusted to a pH of 1.2 at room temperature.

Statement of problem

Photovoltaic clothing requires cells that are flexible and easy to integrate. However most photovoltaic cells are made up of rigid materials like glass panels whose seals can easily break when bent, thus exposing them to air and moisture and destroying their ability to capture energy from the sun. Threads are very flexible, hence solving the cell interconnection problems.

Objective

The main objective of this research is to deposit photoactive WO_3 onto an electrically conductive thread for photovoltaic clothing application. Previous research in our lab made a thread electrode by depositing thin films of tungsten oxide on steel thread; however, no photovoltage was exhibited and this was attributed to the cracks in the film [25].

The specific objectives

i. To determine optimum WO_3 electrodeposition conditions on FTO, a well studied electrode used for this application.
ii. To perform WO_3 electrodeposition on a stainless steel substrate, employing the above and characterizing it using SEM and XRD to determine morphology and crystallinity.
iii. To characterize the photoactivity of the tungsten oxide on stainless steel substrate.
iv. To test tungsten foil for WO_3 deposition and photoactivity.

Significance of the research

The use of electronics in textiles for solar application is being faced with some challenges, such as: cost and reliability. By designing a flexible cell by embedding tungsten oxide on a thread, solar energy could be utilized to generate power. This concept is very useful in off-grid regions, which includes military personnel on remote missions or doctors. They can also provide power during emergencies like hurricanes and earthquakes.

CHAPTER TWO

Experimental

Precursor solution preparation

The precursor solution was prepared by reacting 30% H_2O_2 and 50 mM Na_2WO_4 in a volumetric ratio of 4:1. A pale-yellow solution was initially formed which faded after an hour. Pieces of platinum wire were placed in the solution to decompose the excess hydrogen peroxide. The initial pH of the $Na_2W_2O_{11}$ solution ranged from 8.03 to 9.69; perchloric acid was added dropwise until a pH 1.2 was achieved. The resulting solution was clear. This is shown schematically in figure 6.

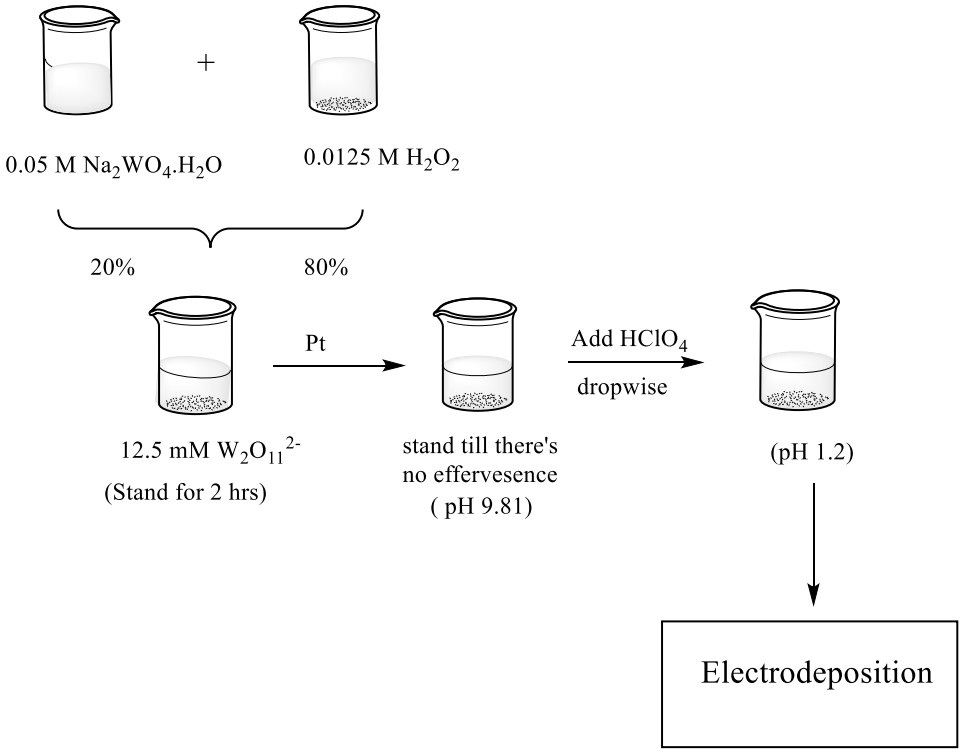

Figure 6: Preparation of the precursor solution

Substrate cleaning procedure

The substrates used as working electrodes for this experiment were: 25mm × 25 mm FTO with a thickness of 2.2 mm, 25 mm ×25 mm stainless steel 304 and the thickness of 0.25 mm and tungsten foil measuring 0.25 mm thick. They were subjected to a cleaning procedure as outlined in figure 7, prior to electrodeposition:

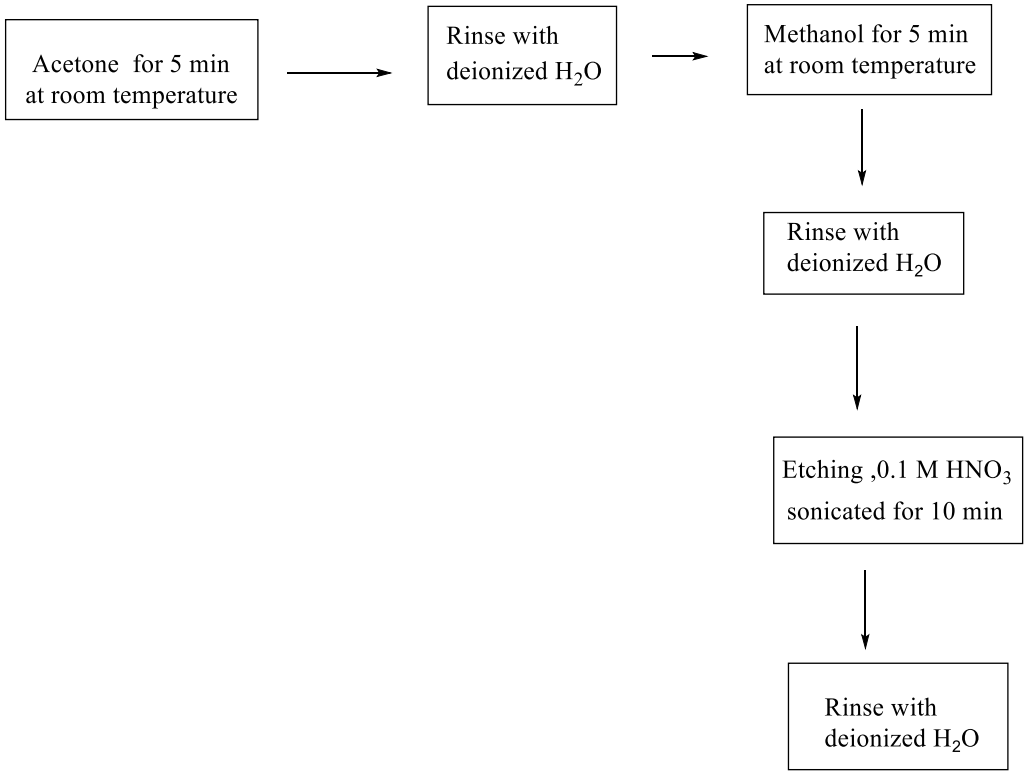

Figure 7: Substrate cleaning procedure

Electrodeposition

Electrodeposition was performed using a Princeton Applied Research (PAR) potentiostat /galvanostat model 273 A in a three electrode Teflon cell (figure 8) with an area of 1.5 cm^2. The reference electrode was Ag/AgCl in saturated KCl and the counter electrode was a platinum wire. The working electrodes were fluorine-doped tin oxide on glass, stainless steel 304 and tungsten foil. All the potentials reported were relative to the reference electrode. The electrodeposition was performed at a potential of -0.5 V for 1.5 h.

Figure 8: Cell diagram used for electrodeposition

Characterization of WO_3 film

An Agilent UV-Vis Spectrophotometer was used to investigate the optical behavior of the films. The UV-Vis absorption spectra of the WO_3 was recorded in the wavelength range from 190-1000 nm. the direct band gap of WO_3 was estimated from Tauc plots of $(\alpha hv)^2$ Vs λ

Where:

$\alpha = 1/d \ln (T/100)$

d= film thickness

T =optical transmittance

h= planck's constant

ν =frequency of light

E_g =optical direct band gap

From the equation

$E = hc/\lambda$

The thicknesses of the films were measured using a TENCOR D-100 profilometer. A JEOL JIB-4500 multi beam system SEM was used to examine the surface morphology of the films deposited on the substrates. The chemical and structural analysis of the samples was done with a Bruker X-ray diffractometer (XRD).

Photoactivity

The same electrochemical system described above was employed for the photoactivity measurements of the films. WO_3 films on FTO substrates and 0.1 M $HClO_4$ aqueous solution (pH = 1) were used as the working electrode and electrolyte, respectively.

The light source was a Newport solar simulator with a 500 W xenon lamp. The measurements were done by measuring the (photo) current while sweeping the potential at a constant scan rate 5 mV/s. This can be done both in the dark and under constant illumination. However, for the W-foil it was performed at a scan rate of 1 mV/s.

CHAPTER THREE

Results and Discussion

Substrates

The precursor solution was electrodeposited on the three substrates: FTO, SS-304 and the W -foil. The influence of two electrodeposition parameters, electrodeposition time and the pH of the precursor solutions, was investigated. The photoactivity of the electrodeposited WO_3 on the three substrates was also determined.

FTO Electrode

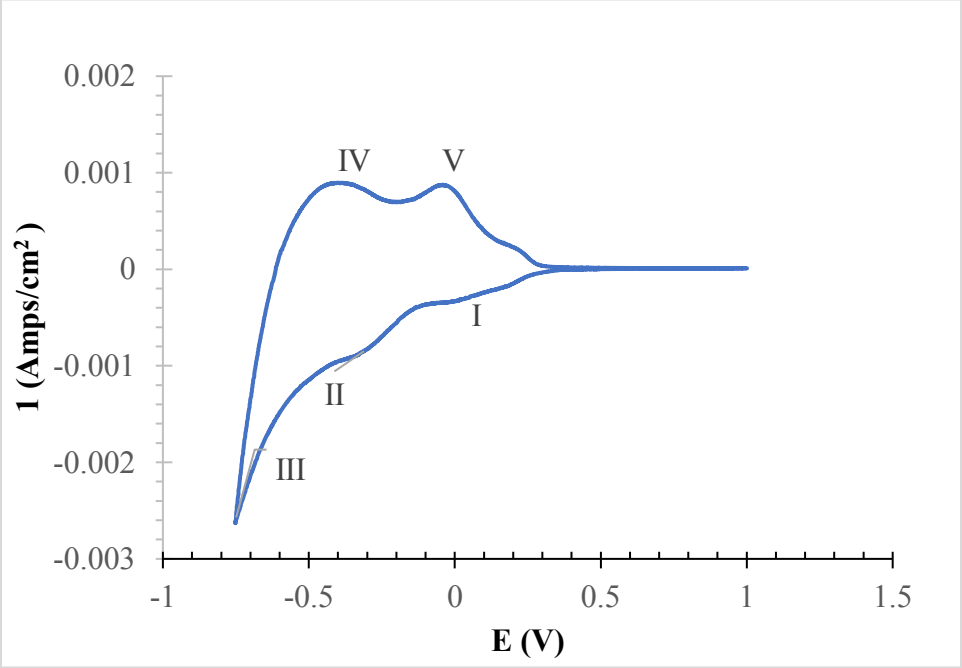

Figure 9 : Cyclic voltammogram of 0.25 mM peroxotungstate solution on FTO

Figure 9 shows a cyclic voltammogram of 12.5 mM peroxotungstate solution on FTO recorded at a potential of -0.7 to 1.0 V vs Ag/AgCl reference electrode at scan rate of 50 mV/s.

It exhibited three cathodic peaks, labelled I, II and III. Peaks I and II were attributed to reduction of tungsten ions to the W^{5+} state. The hydration surrounding the oxide molecules plays a role in the formation of two redox waves for the same process.

Peak III is assigned to hydrogen evolution activity because the potential of the reference electrode used was +0.2 V vs NHE, and the precursor solution was at pH 1.2 .

Effect of $HClO_4$ on FTO

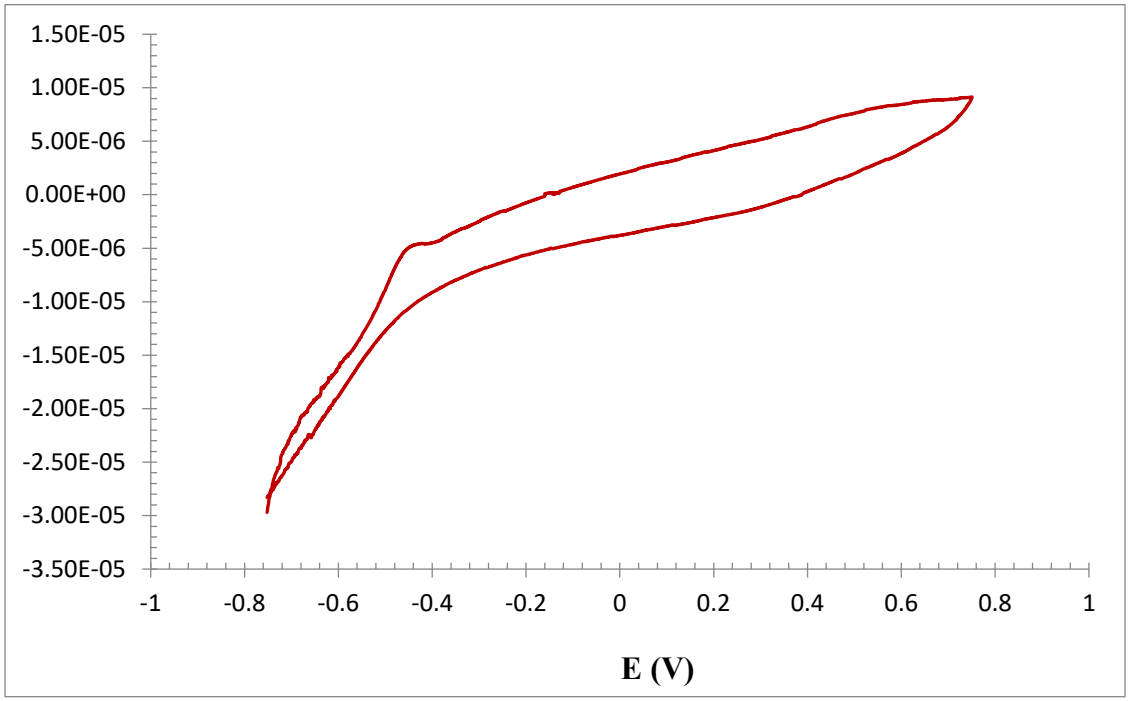

Figure 10: Cyclic voltammogram of 0.1 M $HClO_4$ on FTO recorded at a potential of -0.7 to 1.0 V vs Ag/AgCl at a scan rate of 50 mV/s .

The effect of perchloric acid on FTO was determined by performing a cyclic voltammogram at a potential of -0.7 to 1 V, scan rate of 50 mV/s and 0.1 M $HClO_4$ used as the electrolyte. The voltammogram registered a very small current density of about -3.75×10^{-5} A/cm^2 . The $HClO_4$ had some effect on the FTO electrode. Thus there was a possibility that part of the electrochemistry exhibited by the voltammogram in Figure 10 could be due to perchloric acid.

Effect of H_2O_2 + $HClO_4$ on FTO

The current density of a $HClO_4$ + H_2O_2 voltammogram, as shown in Figure 11, is 10 times more than that of the $HClO_4$ alone (Figure 10). This showed that the H_2O_2 is quite electroactive, so that its removal via catalytic decomposition before the electrodeposition is commenced is imperative. This ensured that the WO_3 deposition reaction was irreversible, since for WO_3 to be oxidized back to $W_2O_{11}^{2-}$, excess H_2O_2 is required, which in this case was decomposed by the platinum wire.

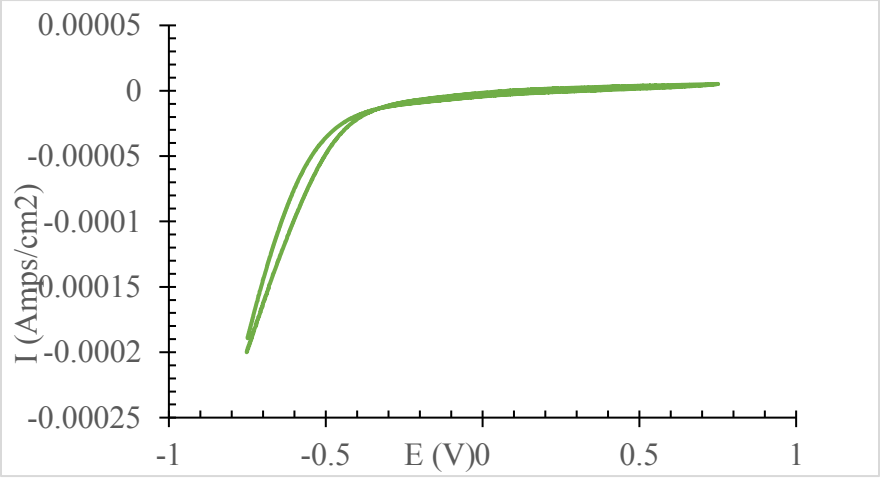

Figure 11: Cyclic voltammogram of 0.1M $HClO_4$ + H_2O_2 on FTO recorded at a potential of -0.7 to 1 V vs Ag/AgCl at a scan rate of 50 mV/s .

Electrodeposition of tungsten oxide on FTO

The electrodeposition solution was prepared as explained in the experimental section. A smooth electrodeposition curve was formed, as shown in Figure 12. A film was formed on the FTO, showing that the electrodeposition of WO_3 on FTO was successful.

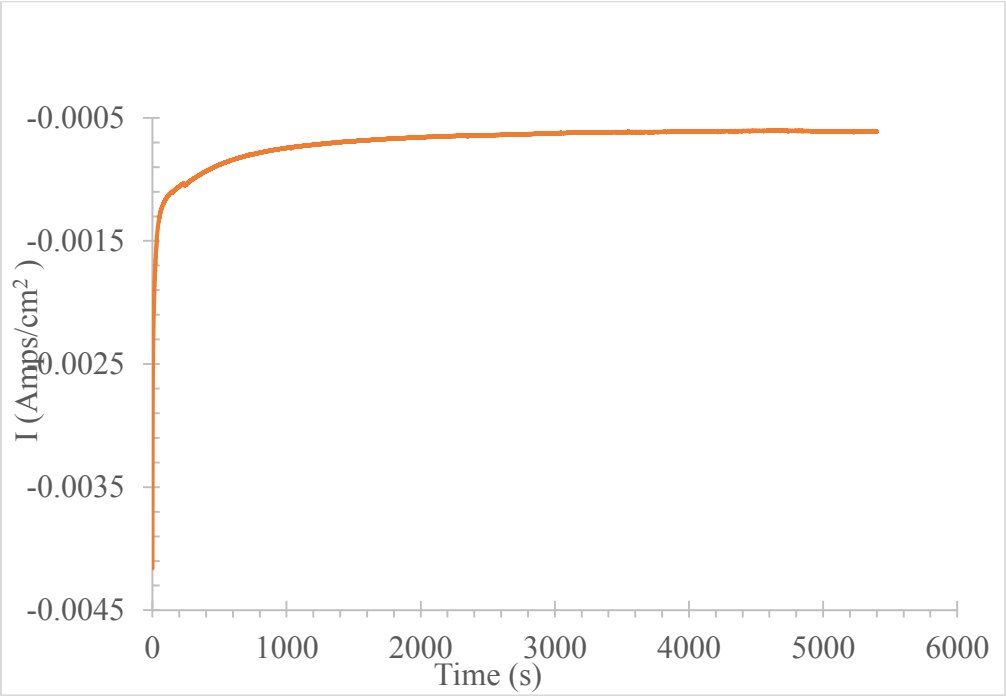

Figure 12 : Electrodeposition curve of WO_3

The film turned blue during the electrodeposition process (Figure 13 (a)) but became yellow/clear after the process (Figure 13 (b)).This is because the film is oxygen sensitive.

(a) (b)

Figure 13 : Electrodeposited film of WO_3 on ITO (a) during electrodeposition process, and (b) minutes after sitting in the air

Electrochromic effect of WO_3 film on FTO

Electrochromism is the reversible change in optical properties of a material when it becomes electrochemically reduced or oxidized [24,26]. Electrochromism was detemined by performing a potentiostatic experiment at -0.3,-0.1 and +0.1 voltages for 1 hour. The electrochemical cell used is the same as described in the experimental section. $HClO_4$ was used as an electrolyte.

At -0.1 V the colour of the film turned into blue; when the potential was changed to +0.1 V the film turned into light yellow. This is attributed to the insertion of protons from the $HClO_4$ into the film. When it is reversed, the protons and electrons are ejected from the tungsten bronze to reform the initial tungsten oxide [24].

$$WO_3 + yH^+ + ye^- \rightleftharpoons H_yWO_3$$

Effects of electrodeposition parameters

The optimum electrodeposition conditions for WO_3 in this work were determined by varying one factor at a time.

pH of precursor solution

The precursor solution was prepared as explained in the experimental section and the pH was varied from 0.8 to 1.2 to 1.8 using 1.0 M $HClO_4$. The solution at pH 0.8 was a colloidal suspension, which formed sediments when it was left to settle, while both pH 1.2 and 1.8 formed a clear solution.

Figure 14 : Electrodeposited films of tungsten in pH (a) 1.8 (b) 1.2 (c) 0.8, respectively

The SEM image of the film from the pH 0.8 solution (Figure 15a) was dense and thick; however, it was not evenly distributed on the FTO substrate. This is because the increase in H^+ concentration caused precipitation of tungsten bronze near the surface of the FTO, resulting in nucleation and growth of WO_3 film, with or without application of external voltage. Film electrodeposited at pH 1.2 (Figure 15b) was smooth and the coverage was even.

The SEM of the pH 1.8 experiment (Figure 15c) shows a thin film. This result was in line with the literature. The pH of solutions between 1.8 and 1.92 produces transparent films, while 0.8 to 1.2 produces mesoporous films [15]. Thus the surface morphology of the WO_3 film is dependent on the pH of the precursor solution.

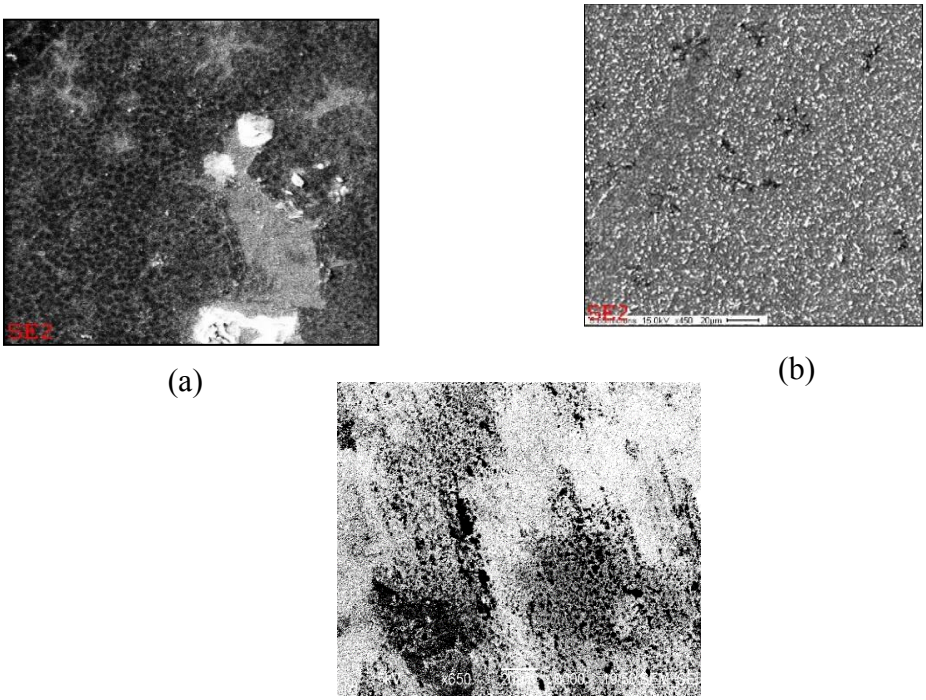

(a) (b)

(c)

Figure 15: SEM images of WO_3 electrodeposited on FTO at the pH of (a) 0.8;(b) 1.2; (c) 1.8.

Electrodeposition time

Figures 16a and b show the SEM of WO_3 films deposited for 1.5 and 3 h, respectivly. The film that was deposited for a 1.5 h had a thickness of 480 nm, while the other one deposited for 3 h had a thickness of 510 nm.

Increasing electrodeposition time allows the reaction of peroxotungstate precursor solution to be electrodeposited until all the peroxo species is used up in the solution. Hence, the thickness of the film increased with increasing deposition time, but not in a linear manner, as the concentration of reagent was steadily decreasing.

The retangular patch seen in Fig. 16b was damage due to prolonged exposure of the ionization beam on one spot during SEM measurements.

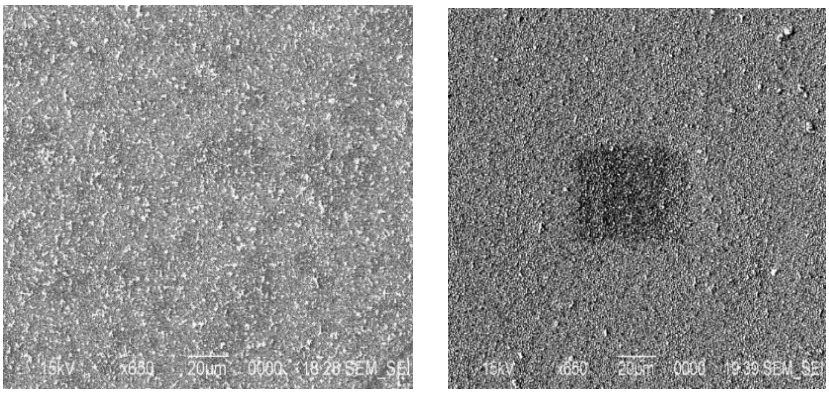

(a) (b)

Figure 16 : WO_3 film electrodeposited on FTO at a potential of -0.5 V for (a) 1.5 and (b) 3 h respectively and annealed at 450 ˚C for 2 h.

The XRD pattern of unannealed WO_3 (WO_3 as electrodeposited) had a broad peak between 23 to 25 degrees, which is a characteristic of the amorphous film. The annealed WO_3 film showed 3 peaks for crystalline planes (002), (020) and (200). Comparing with XRD patterns with the JCPD files, it was consistent with monoclinic structure.

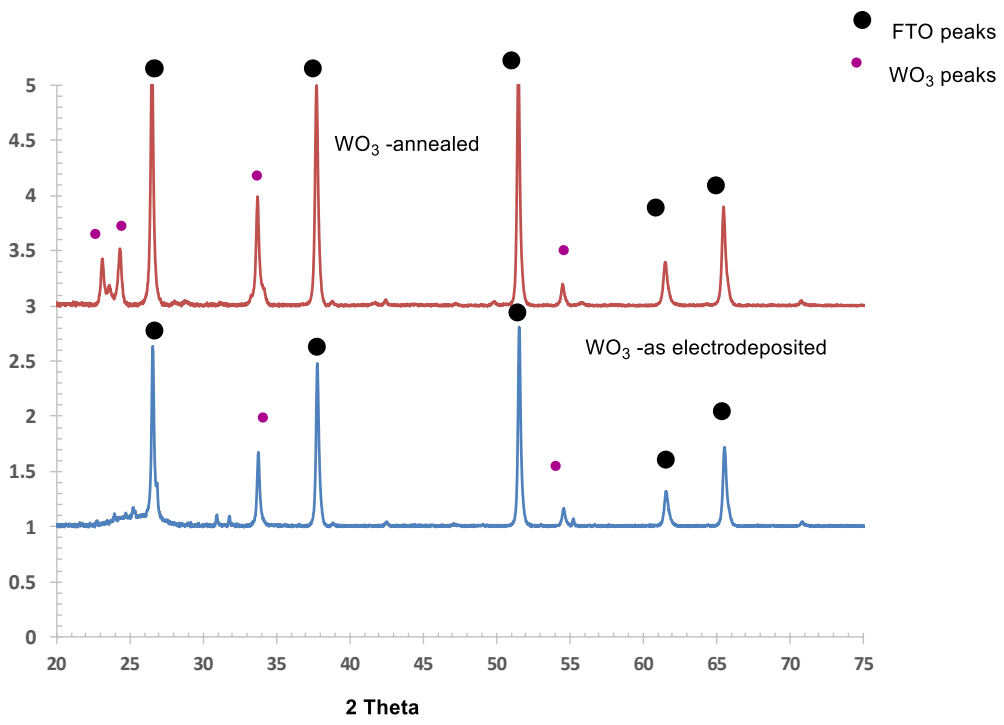

Figure 17: XRD pattern of WO_3 on FTO.

Properties of the electrodeposited WO_3 film on FTO

Throughout this research the electrodeposition parameters of the film were: precursor solution concentration of 25 mM peroxotungstate ions, pH 1.2, electrodeposition time of 1.5 h, and electrodeposition voltage of -0.5 V. The annealing temperature was set to 450 ˚C for 2 h.

Photoactivity

Open-circuit voltage, oxygen evolution and methanol oxidation methods were used to investigate the photoactivity of the film.

The open circuit-voltage method achieved a potential of 89.9 mV and a photocurrent of 0.803 microamps /cm^2.

For oxygen evolution, a typical current-potential curve was obtained, as shown in Figure 18. It resembled that of an n-type semiconductor electrode such as WO_3 on FTO. The onset potential was found to be 0.2 V vs AgCl, which is in line with the onset potential of photoelectrochemical oxygen evolution in the literature for WO_3 [23]. A current of 14.4μA/cm^2 and a voltage of 658 mV was obtained.

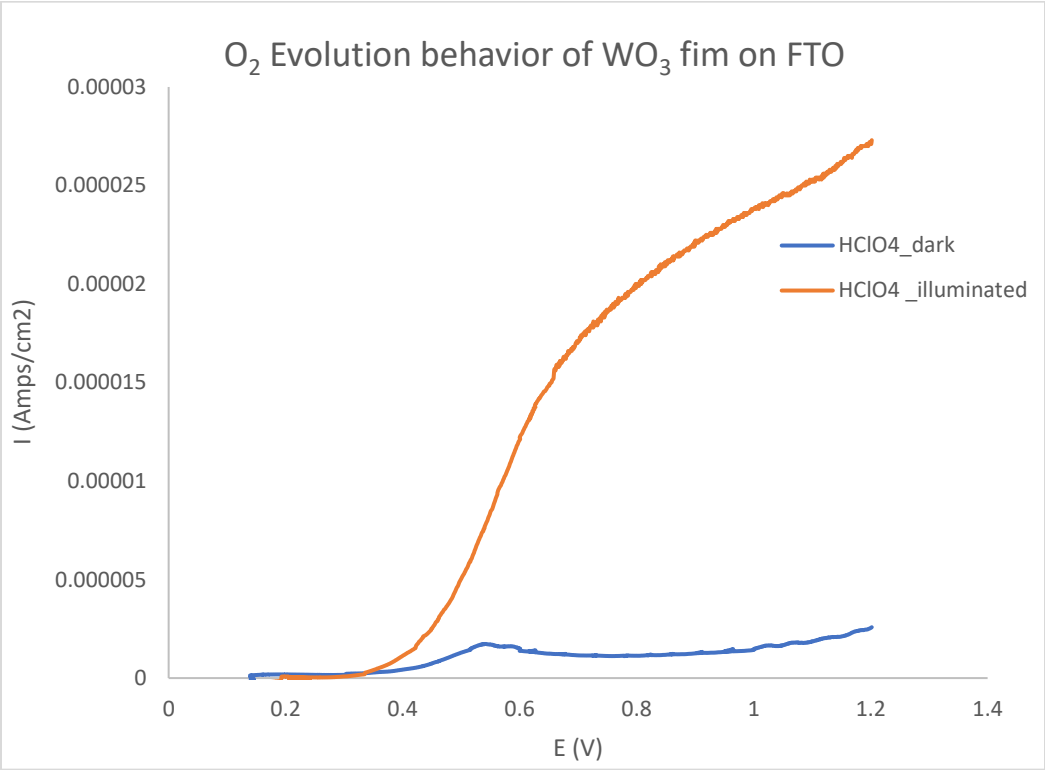

Figure 18: Oxygen evolution behavior of WO_3 on FTO

The addition of methanol as a sacrificial reductant in $HClO_4$ increased the photoresponse of the WO_3 film, as shown in Figure 19. The photocurrent obtained was 57.93 microamps/cm^2 and the voltage was 674 mV. This is about three-fold increase in photocurrent compared to oxygen evolution. This indicated that the current due to photogeneration of CO_2 was augmented by the photooxidation of methanol, which was the dominant process by a factor of two.

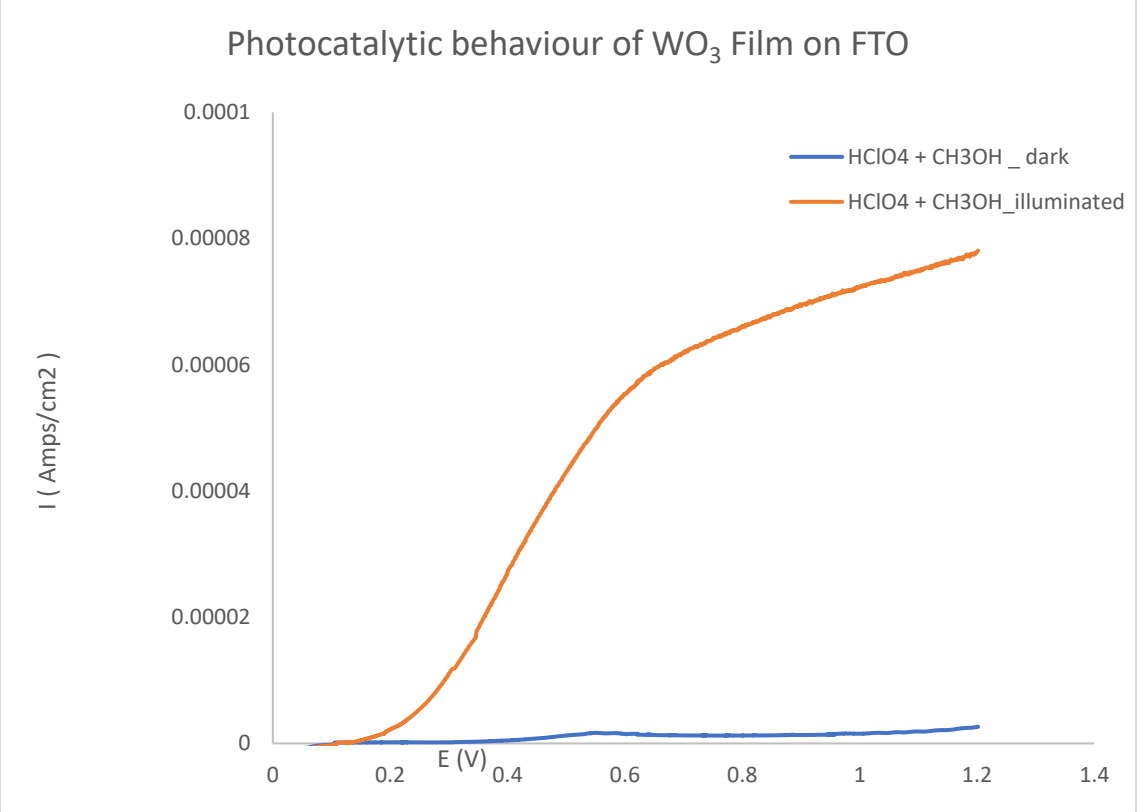

Figure 19 : Photo-oxidation of methanol on WO_3 electrode on FTO

Band gap energy of WO_3 film on FTO

The uv-vis absorption spectrum of WO_3 was recorded in the wavelength range from 190-1000 nm. The direct band gap of WO_3 estimated from a Tauc plot of $(\alpha hv)^2$ vs λ as shown in Figure 20. The band gap energy was calculated to be 2.5 eV, in reasonable agreement with the literature.

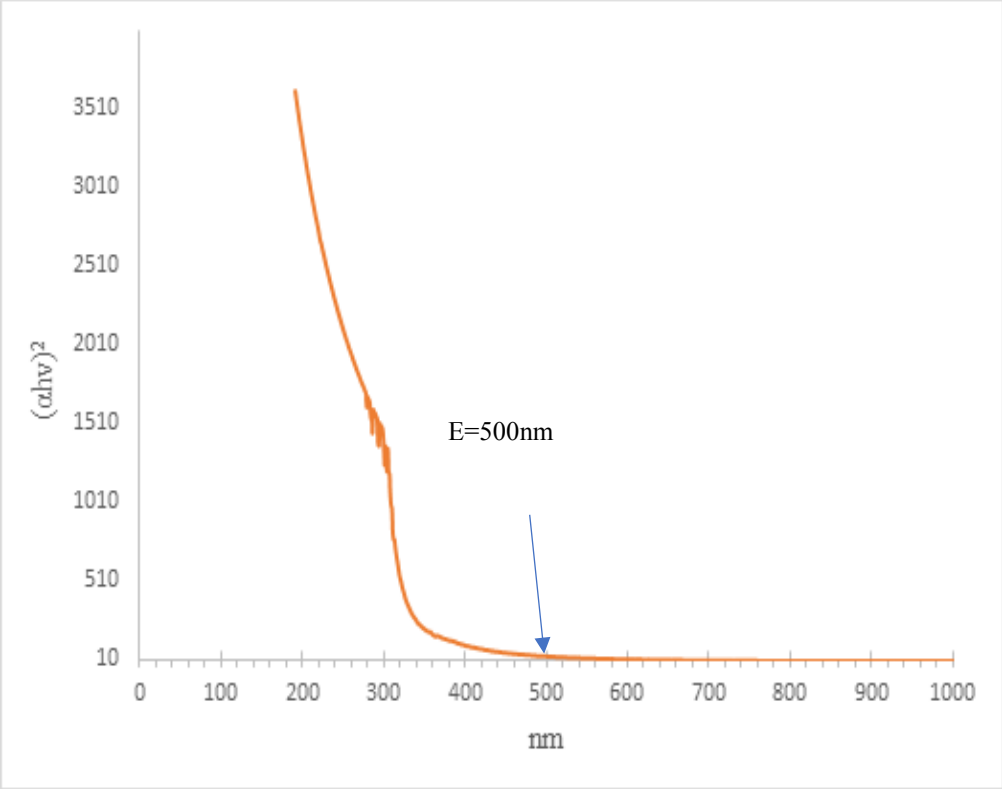

Figure 20 : Determination of band gap energy of WO_3 film on FTO.

Steel substrate

The electrodeposited tungsten oxide on stainless steel was annealed in air at 450 °C for 2 h. The stainless steel turned from shiny metallic to brown, while the blue WO_3 film turned greenish yellow, as shown in Figure 21a and b. This is because the iron underwent oxidation during annealing, and the oxygen content of the WO_3 film rose as well. The SEM image from this sample (Figure 22a) showed some cracks in the film. However, the XRD pattern showed that monoclinic phase of WO_3 was still obtained. There was no photoactivity obtained from this film; instead, it dissolved into the electrolyte (Figure.23a).

(a) (b)

Figure 21 : Electrodeposited WO_3 film on stainless steel-304 (a) as electrodeposited; (b) after annealing in air at 450 °C for 2 h

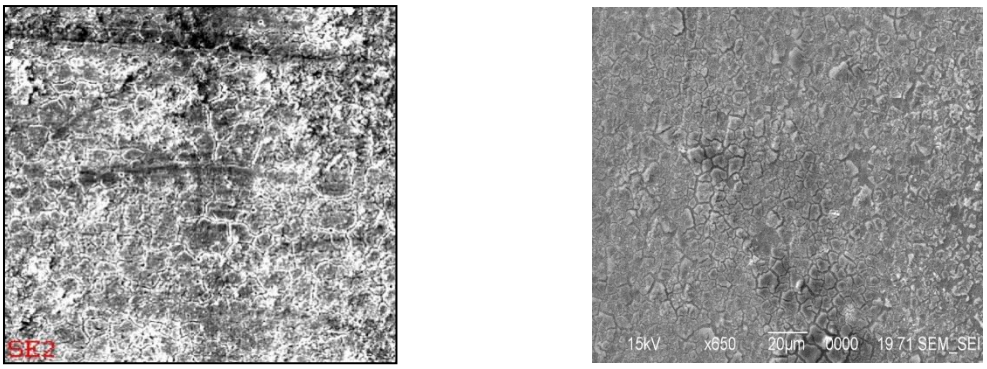

(a) (b)

Figure 22 : SEM images of WO_3 on SS-304 annealed in: (a) air; (b) argon.

The second approach focused on preventing oxidation of the film and the substrate by annealing under argon in the same conditions as stated. Like the previous film, the SEM of the film exhibited some cracking (Figure 22b). Also, the film dissolved in the electrolyte, hence no photoactivity was achieved (Figure 23b).

(a) (b)

Figure 23 : stainless steel substrate after photoactivity measurement (a) annealed in air (b) annealed in argon.

From the Pourbaix diagrams for Fe and W (Figures 24 and 25, respectively), WO_3 is stable at pH < 3. However, for stainless steel, which is made up mostly of iron, the thermodynamics are opposite to that of tungsten. For instance, iron is oxidized to Fe^{2+} at pH < 4. This results in corrosion. This is the reason why the film was dissolved; given that the electrolyte was at pH 1 the Fe dissolved away from underneath the WO_3 film and thus no photovoltage was possible.

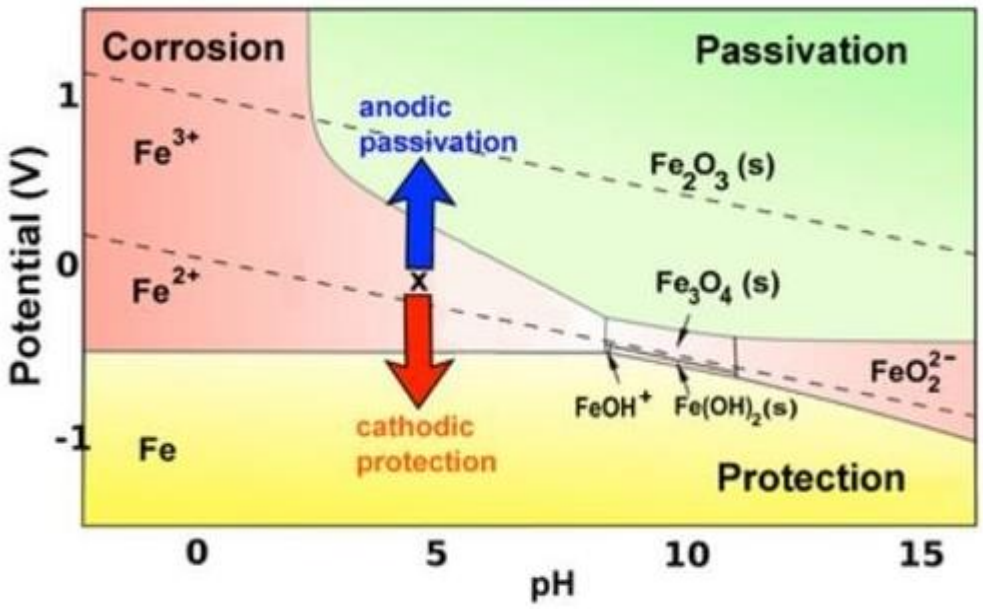

Figure 24 : Pourbaix diagram for Iron [27].

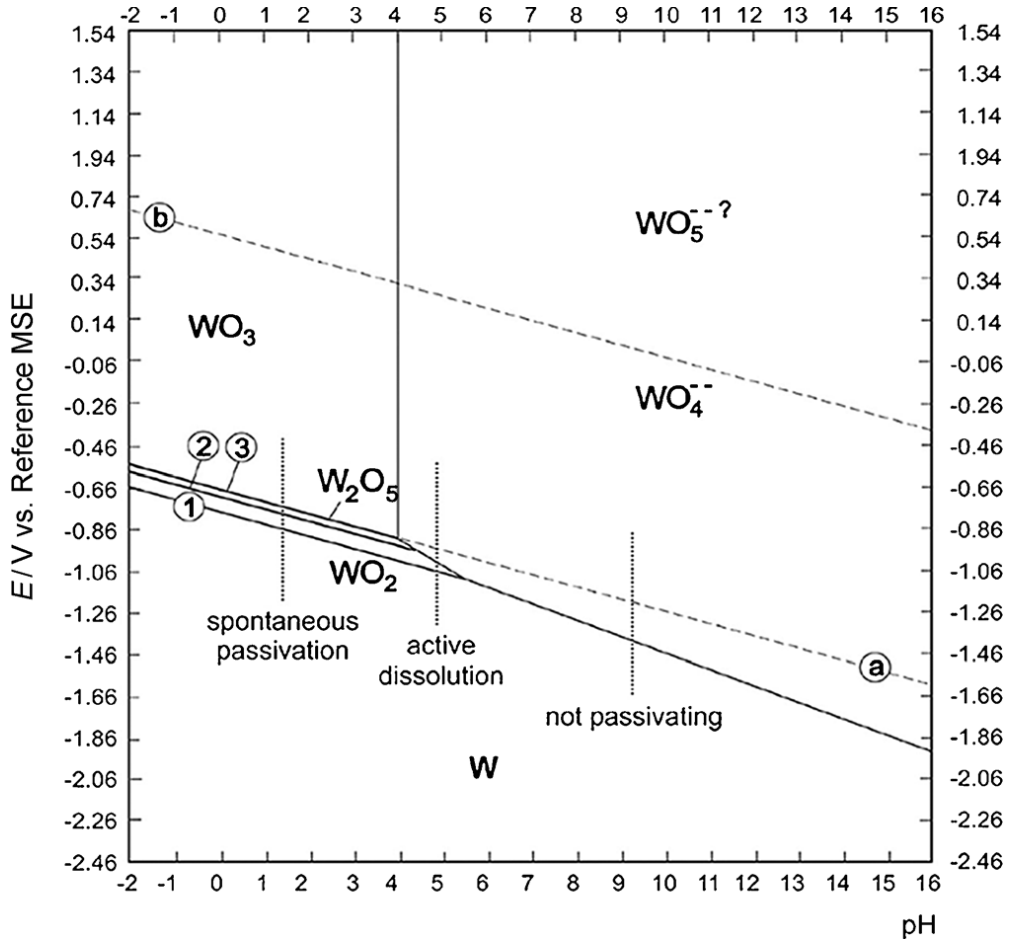

Figure 25 :Pourbaix diagram for W [19].

W foil substrate

WO_3 was electrodeposited on the tungsten foil. One sample was annealed in oxygen (Figure 26(a)) and the other in argon (Figure 26(b)). The annealing conditions were as outlined in the experimental section.

(a) (b)

Figure 26 : Electrodeposited WO_3 on W-foil (a) annealed in air (b) annealed in argon

The SEM of the sample annealed in argon had some cracks, as shown in Figure 27a. From this study, annealing of tungsten oxide in an inert environment causes deprivation of oxygen molecules, hence causing a deviation from stoichiometry thus, cracking. The electrode did not show any photoactivity for both open circuit light/dark measurements and oxygen evolution. This was attributed to the cracks on the film

The second approach was to anneal the sample in air. SEM images from the sample subjected to annealing in air showed a smooth film, as show in Figure 27b.

Photoactivity measurements were performed using the following methods: open circuit-light/dark measurements, oxygen evolution and methanol oxidation.

The electrode was unable to register any voltage or current using the open-circuit-light/dark measurement method.

Oxygen evolution method produced a photocurrent of 39.3 μA/cm^2 and a voltage of 971 mV. Methanol oxidation registered a photocurrent of 69.07 μA/cm^2 and a voltage of 964 mV. The flat band potential for oxygen evolution was +0.5 V versus AgCl. When methanol was added to the electrolyte the amount of current recorded was higher than that of the electrolyte solution by itself (Figure 28). This is consistent with what was seen for the FTO electrode. The XRD patterns of both approaches were monoclinic

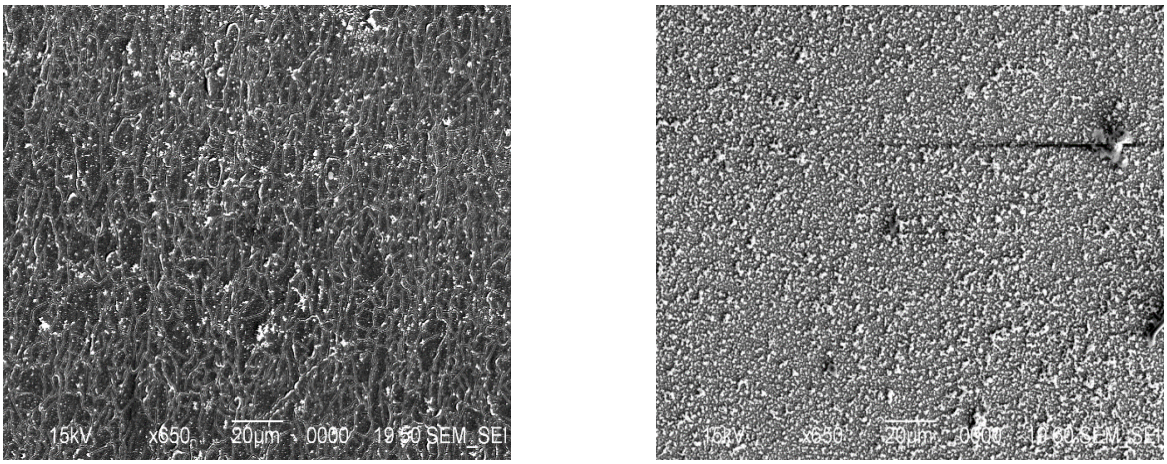

(a) (b)

Figure 27 : WO_3 on W foil annealed at 450 °C for 2 hours in: (a) Ar; and (b) air.

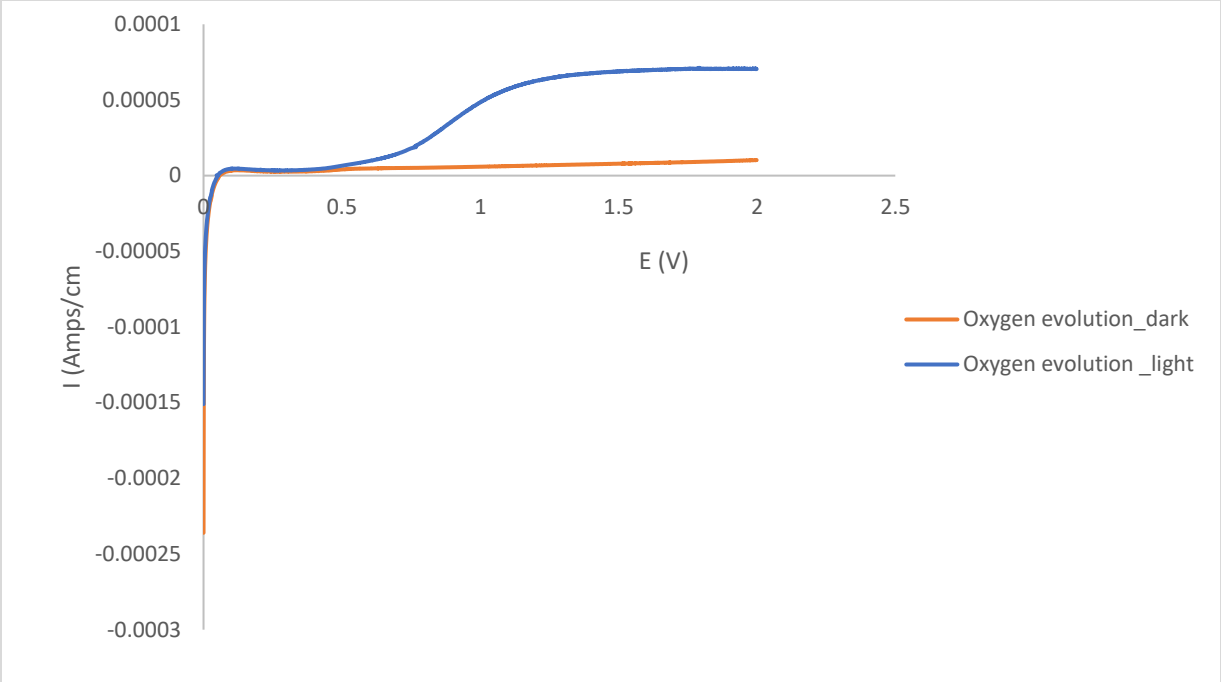

Figure 28: Oxygen evolution behavior of WO_3 on W-foil

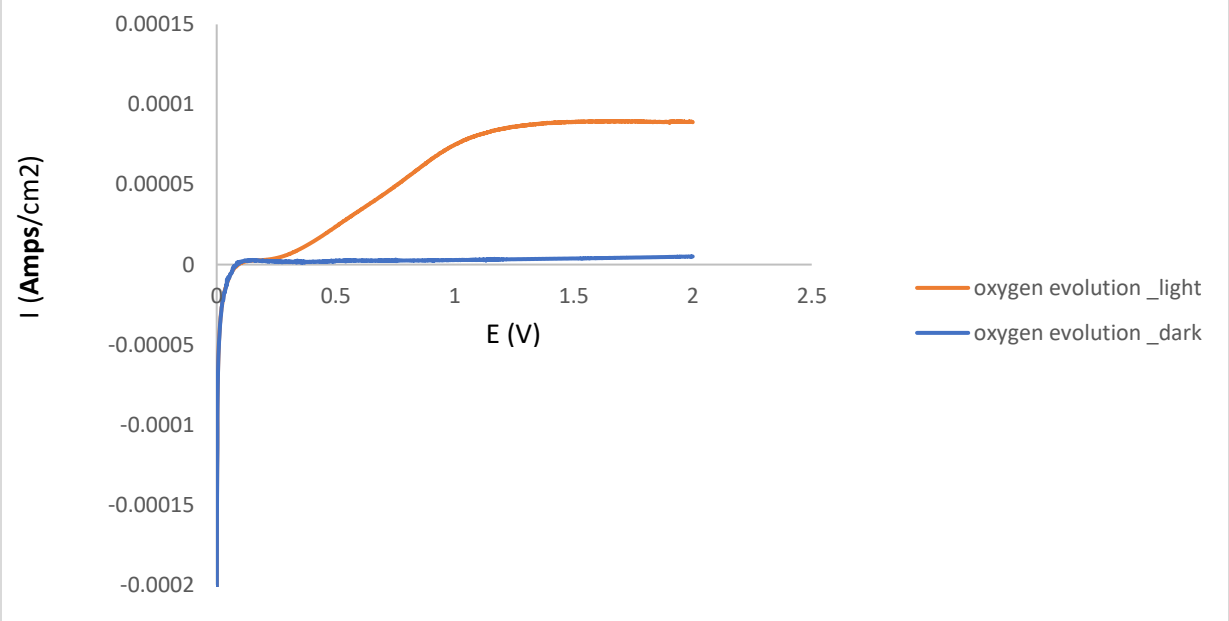

Figure 29 : Photo-oxidation of methanol on WO_3 electrode on W-foil.

CHAPTER FOUR

Conclusion

Tungsten oxide thin films were successfully electrodeposited via reduction of peroxotungstate ion on three substrates: FTO, stainless steel and tungsten foil. Excess hydrogen peroxide in the electrolyte was decomposed using a platinum wire. The XRD study showed that the electrodeposited tungsten oxide was amorphous, which changed into monoclinic upon annealing at 450 ^{o}C. The morphology of the film depended on the pH of the precursor solution. A pH 1.2 electrolyte produced a smooth film as observed under the SEM. Using the oxygen evolution method, a photocurrent of 14.4 $\mu A/cm^2$ and a voltage of 658 mV for the tungsten oxide films on FTO was observed. For the W foil substrate, the WO_3 film was able to register a photocurrent of 39.3 $\mu A/cm^2$ and a voltage of 964 mV photoactivity. Using the FTO substrate, the band gap energy of the electrodeposited film was found to be 2.5 eV. The film on stainless steel did not exhibit any photoactivity; instead, it disolved into the electrolyte. This shows that the behavior of the substrate on different pH conditions should be taken into consideration for photovoltaic applications.

The next generation of photovoltaic clothing and other woven fiber applications require semiconductor deposition on a thread substrate to be effective. The tungsten foil gave positive results in terms of photoactivity. Hence, the next step can explore on the tungsten thread while checking on ways to improve its photoactivity**.**

References

[1] N. Z. Muradov and T. N. Veziroğlu, "'Green' path from fossil-based to hydrogen economy: An overview of carbon-neutral technologies," *International Journal of Hydrogen Energy*. 2008.

[2] P. A. Owusu and S. Asumadu-Sarkodie, "A review of renewable energy sources, sustainability issues and climate change mitigation," *Cogent Engineering*. 2016.

[3] NREL, "Best Research-Cell Efficiency Chart | Photovoltaic Research | NREL," *Best Research-Cell Efficiency Chart | Photovoltaic Research | NREL*, 2019. .

[4] A. J. Nozik and J. Miller, "Introduction to solar photon conversion," *Chemical Reviews*. 2010.

[5] A. Rothwarf and K. W. Böer, "Direct conversion of solar energy through photovoltaic cells," *Prog. Solid State Chem.*, 1975.

[6] M. Grätzel, "Photoelectrochemical cells," *Nature*. 2001.

[7] B. Zaidi, "Introductory Chapter: Introduction to Photovoltaic Effect," in *Solar Panels and Photovoltaic Materials*, 2018.

[8] H. P. Mahabaduge *et al.*, "High-efficiency, flexible CdTe solar cells on ultra-thin glass substrates," *Appl. Phys. Lett.*, 2015.

[9] M. Ravindiran and C. Praveenkumar, "Status review and the future prospects of CZTS based solar cell – A novel approach on the device

structure and material modeling for CZTS based photovoltaic device," *Renewable and Sustainable Energy Reviews*. 2018.

[10] Y. Xu, T. Gong, and J. N. Munday, "The generalized Shockley-Queisser limit for nanostructured solar cells," *Sci. Rep.*, 2015.

[11] R. R. Mather and J. I. B. Wilson, "Fabrication of photovoltaic textiles," *Coatings*. 2017.

[12] G. Cho and A. Han, "Review of performance evaluation on e-textiles and textile-based keypads," *Int. J. Fash. Des. Technol. Educ.*, 2011.

[13] H. Zheng, J. Z. Ou, M. S. Strano, R. B. Kaner, A. Mitchell, and K. Kalantar-Zadeh, "Nanostructured tungsten oxide - Properties, synthesis, and applications," *Adv. Funct. Mater.*, 2011.

[14] J. W. J. Hamilton, J. A. Byrne, P. S. M. Dunlop, and N. M. D. Brown, "Photo-oxidation of water using nanocrystalline tungsten oxide under visible light," *Int. J. Photoenergy*, 2008.

[15] B. Yang, H. Li, M. Blackford, and V. Luca, "Novel low density mesoporous WO3 films prepared by electrodeposition," *Curr. Appl. Phys.*, 2006.

[16] A. W. Bott, "Electrochemistry of Electrochemistry of Semiconductors," *Curr. Sep.*, 1998.

[17] M. Gillet, K. Aguir, C. Lemire, E. Gillet, and K. Schierbaum, "The structure and electrical conductivity of vacuum-annealed WO3 thin films,"

Thin Solid Films, 2004.

[18] V. O. Makarov and M. Trontelj, "Sintering and Electrical Conductivity of Doped WO3," *J. Eur. Ceram. Soc.*, 1996.

[19] T. Zhu, M. N. Chong, and E. S. Chan, "Nanostructured tungsten trioxide thin films synthesized for photoelectrocatalytic water oxidation: A review," *ChemSusChem*. 2014.

[20] L. Lin, C. P. Cheng, and T. P. Teng, "Electrodeposition-Based Fabrication and Characteristics of Tungsten Trioxide Thin Film," *J. Nanomater.*, 2016.

[21] K. Yamanaka, "Electrodeposited films from aqueous tungstic acid-hydrogen peroxide solutions for electrochromic display devices," *Jpn. J. Appl. Phys.*, 1987.

[22] P. K. Shen, A. C. C. Tseung, and H. T. Huang, "A Study of Tungsten Trioxide and Polyaniline Composite Films: I. Electrochemical and Electrochromic Behavior," *J. Electrochem. Soc.*, 1992.

[23] S. H. Baeck, T. Jaramillo, G. D. Stucky, and E. W. McFarland, "Controlled Electrodeposition of Nanoparticulate Tungsten Oxide," *Nano Lett.*, 2002.

[24] T. Pauporté, "A Simplified Method for WO[sub 3] Electrodeposition," *J. Electrochem. Soc.*, 2002.

[25] L. Munoz, "Electrochemical Method for Fabrication of Photovoltaic Fibers based on Tungsten Oxide," Youngstown state University, 2019.

[26] P. K. Shen and A. C. C. Tseung, "Study of electrodeposited tungsten

trioxide thin films," *J. Mater. Chem.*, 1992.

[27] W. G. Cook and R. P. Olive, "Pourbaix diagrams for the iron-water system extended to high-subcritical and low-supercritical conditions," *Corros. Sci.*, 2012.